Statistical physics of the Schelling model of segregation

Author: Sintayehu Andreu Sanchez
Facultat de Física, Universitat de Barcelona, Diagonal 645, 08028 Barcelona, Spain.

Advisor: Emanuele Cozzo

This paper explores the 1D Schelling model's statistical physics, focusing on segregation and unhappiness coefficients across varied vacancy densities and magnetization values. Derived from the interdisciplinary field of Sociophysics, the 1D variant offers computational efficiency. The study reveals increasing segregation with rising vacancy density, emphasizing potential second-order transitions. Unhappiness decreases with more vacancies, displaying abrupt yet continuous shifts, suggesting potential phase transitions. Finite-size effects underscore the need for larger grid simulations. These findings provide a foundation for deeper investigations into Schelling model dynamics and phase transitions in diverse scenarios.

I. INTRODUCTION

In the ever-evolving landscape of interdisciplinary research, the fusion of physics and sociology has given rise to a burgeoning field known as Sociophysics [1]. A notable precursor to this approach is the Ising model, conceived by Ernst Ising. Originally designed as an abstract spin system, the Ising model has proven instrumental in inspiring the development of general self-organization models. These models, though inherently simplified, have been applied to investigate various social dynamics, including opinion evolution, migration patterns, and language evolution.

In this class of models, the Schelling model, introduced by economist Thomas Schelling [2]], has garnered significant attention for its exploration of segregation dynamics within social systems. As highlighted in [4], it shares a relation with the Bluem-Capel model in the realm of physical models, albeit differing in dimension.

The Schelling model is usually introduced as a 2D-lattice model with dimensions $L \times L$ [3]. In this model, each site can exist in one of three states: 0 denotes a vacancy, while ± 1 represent two types of agents. These agents are distributed randomly with densities ρ_0 and $\rho_\pm$, respectively. Every agent is assigned a tolerance number, denoted as T, which indicates the maximum number of agents of the opposite type allowed in their Moore neighborhood (including up, down, left, right, and both diagonals) for them to be considered unhappy.

From an agent's perspective, a sensible tolerance value could be $T = 1/2$. This implies that an agent is content with having half of its neighbors of the same type, reflecting a desire to attain a system that maximizes diversity. The model then identifies unhappy agents based on the established conditions and attempts to relocate them to a position where they could be happy.

Exploring less constrained variations of the model, as exemplified in [4], introduces a scenario where not only unhappy agents can be moved, but also happy agents, provided their happiness does not diminish. This type of movement introduces a noise element, potentially preventing the formation of large but finite clusters that hinder true large-scale segregation.

The resulting states may include frozen states or stationary states, contingent on whether only unhappy agents can be moved or if any agent can be relocated, given that their happiness remains unaltered. Surprisingly, for the specified tolerance value, the model yields an unexpectedly highly segregated state. Delving into variations in vacancy density, ρ_0, and tolerance, T, unveils diverse and intriguing situations warranting further exploration.

The investigation conducted in [4] reveals that segregation undergoes a second-order phase transition at a critical value of T. For low tolerances, only a few sites exist where an agent could be surrounded by a high majority of its own agent type, resulting in a frozen state reminiscent of the randomly generated initial state, with a majority of agents remaining unhappy.

Conversely, a high tolerance scenario results in a mixed stationary state, as agents are indifferent to the types of neighbors they have. Lastly, moderate tolerance values predominantly lead to segregated stationary states, which can manifest as either compact or diluted states contingent upon the density of vacancies.

The 2D-grid model discussed here is versatile in representing various scenarios within a distributed two-dimensional space, such as a city or neighborhood. However, there is merit in exploring the 1D version of this model, as done by Schelling in his model introduction of it [2].

An illustrative instance of a one-dimensional scenario is a classroom, where the initial impression might suggest a 2D layout, but in reality, a student's interactions are limited to their left and right neighbors, reducing it to a 1D problem. Due to the computational efficiency and lower optimization requirements associated with one dimension, this work focuses on investigating and analyzing the dynamics of the model in one dimension.

II. 1D MODEL

A. Order parameters

This model can be examined through two different order parameters: system unhappiness u and segregation s. Let's begin by investigating how the overall system unhappiness responds to variations in vacancy density ρ_0 and magnetization $m = \rho_+ - \rho_-$. We will follow the queuing method, as detailed in [5] for a tolerance of $T = 1/2$. The queuing method, as outlined in [5], involves certain approximations concerning the real dynamics. For instance, instead of randomly selecting agents based on whether to jump or not, the method assumes the implementation of an intelligent algorithm that maximizes the results of the optimization process.

They consider the case where $m \geq 0$, signifying an abundance of + agents compared to − agents. Starting with a randomly distributed grid, the fraction of unhappy agents can be calculated as:

$$\rho_{\pm}^{U} = \rho_{\pm}\rho_{\mp}^{2} \tag{1}$$

It is noteworthy that, on average, the initial number of unhappy minority − agents surpasses the count of unhappy majority + agents. Now, let's explore the queuing approach. In this scenario of a random distribution, if there exists a single vacancy favorable for a + agent, an unhappy + agent will be relocated to that vacancy. In this version of the model, a + agent becomes unhappy only if its immediate surroundings follow the sequence $-+-$; when the + agent moves, it leaves behind a vacancy friendly for a − agent, creating a vacancy for a subsequent + agent, and so forth. This process continues until all the majority unhappy agents have been relocated to happy environments. At this juncture, the unhappiness value is given by $u_\infty = \rho_-^U - \rho_+^U$.

The unhappy − agents may enhance their situation if there are appropriate vacancies available in the system. The count of these vacancies, which are favorable for − agents, can be determined as follows:

$$\rho_V^{F-} = \rho_o(1 - \rho_+^2) \tag{2}$$

Considering all factors, the ultimate number of unhappy agents in the final frozen state is determined by:

$$u_\infty = \rho_-^U - \rho_+^U - \rho_V^{F-} \tag{3}$$

As previously mentioned, these are the calculations used for the [5] model. However, in our context, both + and − agents will experience unhappiness in the situation $0 \pm \mp$. Accounting for this, the potential vacancies for the remaining − agents are determined by:

$$\rho_V^{F-} = \rho_o(1 - \rho_+^2 - 2\rho_o\rho_+) \tag{4}$$

The study of equation (3) provides insights into a notable shift in the unhappiness behavior with increasing vacancy density. This observed alteration, characterized by its continuous nature, suggests the potential occurrence of a second-order phase transition

Concluding the examination of the system's unhappiness, it is crucial to recognize that this analysis is an approximation. As previously mentioned, it relies on an intelligent algorithm rather than random selection when deciding which agent should be moved. Moreover, these calculations overlook the potential impact of moving one unhappy agent on the happiness state of its neighbors, both past and future. Considering these factors, the actual values of overall unhappiness might deviate slightly from the approximation.

Prior to delving into the details of the simulation, considering the physics-oriented perspective of this model, it is imperative to discuss phase transitions. For this purpose, we have adhered to the concepts elucidated in [6]. They elaborate on the utilization of the partition function $\mathcal{Z}_N$ and the computation of entropy to compute unhappiness values of final frozen states. Upon scrutinizing unhappiness, one observes that, for a particular vacancy density denoted as ρ_0^*, a first-order phase transition occurs, causing the unhappiness value to plummet abruptly to zero.

To assess segregation in our analysis, we employ a methodology inspired by the approach outlined in [4]. A cluster is defined as a group of agents of the same type, ranging from a single-agent group to a group comprising $N\pm$ agents. In their investigation, they introduce a weighted sum of the final configuration's cluster sizes, denoted as $S = \sum_c n_c p_c$. Here, n_c represents the cluster size, and $p_c = n_c/N_{\text{agents}}$ serves as the weight of the cluster. This value is normalized with respect to the maximum size a cluster could achieve, specifically in the scenario where the magnetization is $m = 0$, resulting in normalization by $N_{\text{agents}}/2$. Noteworthy is the consideration that $N_{\text{agents}} = N(1-\rho_0)$, leading to the expression:

$$s = \frac{2}{(N^2(1-\rho))^2}\sum_c n_c^2 \tag{5}$$

When accounting for different magnetization values, proper normalization of S involves dividing the + agents clusters by their maximum value N_+ and the − agents clusters by N_-, resulting in:

$$s = \frac{\sum_{\{c_+\}} n_{c_+}^2}{N(1-\rho_o)N_+} + \frac{\sum_{\{c_-\}} n_{c_-}^2}{N(1-\rho_o)N_-} \tag{6}$$

Regarding segregation, some preliminary steps must be considered before utilizing Equation 6. Similar to the approach in [4], a real space re-normalization of the grid is necessary to ensure that segregation values do not dilute excessively in cases of high vacancy density. In our 1D model, re-normalization is relatively straightforward; all that is needed is to remove all vacancies from the grid.

B. Simulations

In our simulations, we have employed a 1D model featuring periodic boundary conditions and interactions with first neighbors. The primary constraint imposed is that only unhappy agents are eligible for movement. Given the nature of a 1D lattice, the tolerance of any agent can be either $T = 1/2$ or $T \leq 1/2$. In this case, the former option has been selected. Notably, this tolerance value is computed exclusively based on the agent sites. To elaborate, in scenarios where an agent's vicinity comprises a vacancy and an agent, the agent alone is considered for tolerance computation. Consequently, an agent is deemed unhappy if both neighbors are of a different type or if one neighbor is a different type of agent and the other is a vacancy. For instance, a + agent experiences unhappiness in situations such as $0+-$, $-+0$, and $-+-$, while it is happy in scenarios like $+++$, $++0$, $0++$, $-++$ and $++-$.

The simulation employed in this project initiates with an N-sites lattice featuring N_+ + agents and N_- − agents, determined by the vacancy density ρ_0 and the magnetization m, randomly distributed (as depicted on the left side of Fig.1). The maximal number of vacancy densities that can be studied is determined by the value m, as $N_- = (1 - \rho_o - m)/2$ have to be bigger than zero. At each step, the algorithm identifies unhappy agents in their current positions and randomly selects one of them. For the chosen agent, it evaluates all vacancies to determine which one could potentially make the chosen agent happy and randomly selects one such vacancy. If no suitable vacancy is found, the process is repeated with another agent of the opposite type until one can be relocated. Each step concludes with the movement of a single agent.

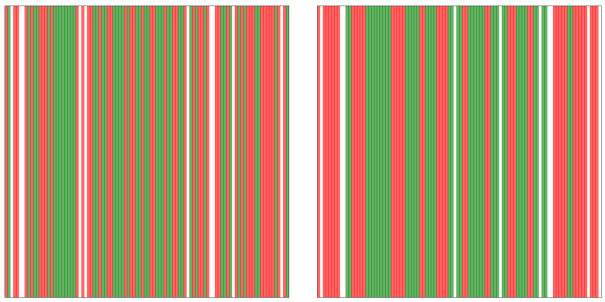

FIG. 1: Example of agents distribution through the lattice for a $N = 100$ sites lattice, a magnetization $m = 0$ and vacancy density $\rho_o = 0.1$, each vertical line represent an agent. On the left there is the initial randomized distribution. On the right there is the final frozen state where the segregation can be easily seen.

The simulation terminates either when there are no more unhappy agents or when there are no suitable vacancies for any unhappy agent. The final state attained is a frozen state, implying that no agents can be moved, and either all agents are happy, or there are some agents who would remain unhappy in any remaining vacancy (right side of Fig.1).

Upon reaching a frozen state, the subsequent step involves calculating the segregation and overall unhappiness of this state. To compute unhappiness, the program sums the number of agents still situated in unhappy sites and normalizes it by the total number of agents. For the segregation, With the re-normalization completed, the program simply needs to sum the number of agents in each cluster and apply Equation (6).

This entire process constitutes the simulation of one initial scenario for a given set of parameters: N, ρ_0, and m. Leveraging the computational power of the project's computers, the simulation was averaged 100 times for every combination of N, ρ_0, and m. The error of this averaged study is determined by its variance, denoted as σ^2, calculated by $\sigma^2 = \langle s^2 \rangle - \langle s \rangle^2$ and $\sigma^2 = \langle u^2 \rangle - \langle u \rangle^2$.

The values explored for N and m are within the sets $N \in \{100, 500, 1000, 2000, 3000\}$ and $m \in \{0.0, 0.2, 0.4\}$. These values have been computed for 80 values of ρ_0 within the range $\rho_0 \in [0.01, 0.8)$. There is one exception for the value $m = 0.4$, as per its definition, ρ_0 can only reach 0.59 if non-negative values of − agents are to be accommodated.

III. RESULTS

A. Segregation

Starting with the results pertaining to the segregation coefficient $\langle s \rangle$, as depicted in Fig. 2, it is evident that segregation tends to rise with an increase in the number of vacancies. This phenomenon may be attributed to the growing opportunities for agents to find adjacent sites with the same agent type, fostering happiness.

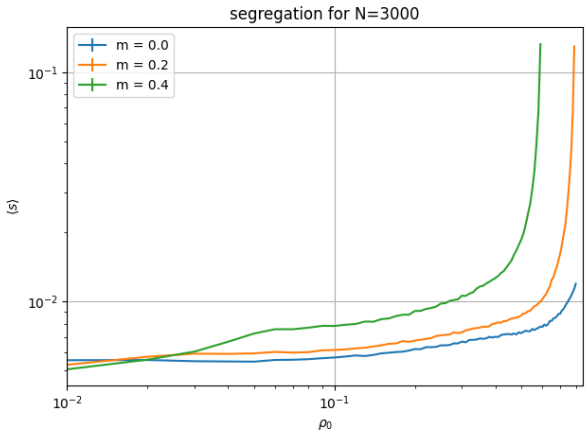

FIG. 2: Capturing the dynamics of the segregation coefficient as a function of various vacancy densities, with a constant grid size of $N = 300$, across diverse magnetization values m. Both axis are presented in logarithmic scale.

For magnetization values other than $m = 0$, the segregation undergoes significant escalation. This phenomenon can be elucidated by the fact that, with an increase in vacancies, minority agents tend to form a single or limited number of clusters due to their scarcity. This effect becomes more pronounced with a reduction in the grid length. For instance, in Fig. 3, the segregation for $N = 100$ reaches $s = 1$ at $\rho_0 = 0.58$ and $\rho_0 = 0.59$, wherein only one minority agent create one cluster. During re-normalization, only two clusters endure. To see this effect for bigger size grids, a closer value to $\rho_o = 0.6$ will be required. Form magnetization $m = 0$, as the number of agents is the same for each type no such behavior is present.

The impact of finite-size grids is evident in Fig. 3. With an increase in the number of sites in the grid, the segregation value diminishes. While it might initially appear that the segregation reaches a certain value as the grid size expands, definitive conclusions regarding finite-size effects cannot be drawn, as the largest studied number may still not be sufficiently large.

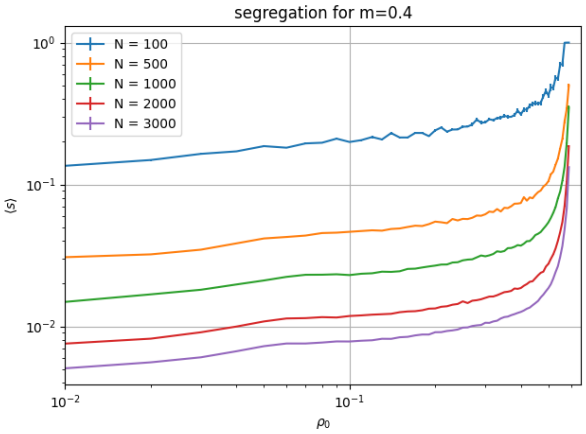

FIG. 3: Capturing the dynamics of the segregation coefficient as a function of vacancy densities, with a constant magnetization value of $m = 0.4$, across diverse grid sizes denoted by N. Both axis are presented in logarithmic scale.

As previously mentioned, there exists a substantial disparity in the values of the segregation coefficient between small and large vacancy densities. This shift in behavior is both abrupt and continuous, potentially indicating the presence of a second-order transition. To ascertain whether this signifies a phase transition, a more thorough investigation of its behavior is imperative.

B. Unhappiness

Now, let's delve into the behavior of the unhappiness coefficient $\langle u \rangle$. Examining Fig. 4, it is evident that the unhappiness values approach zero as the number of vacancies increases. This occurrence is a result of more sites becoming available for an unhappy agent to move, rapidly diminishing the probability that none of these sites will be suitable for relocation.

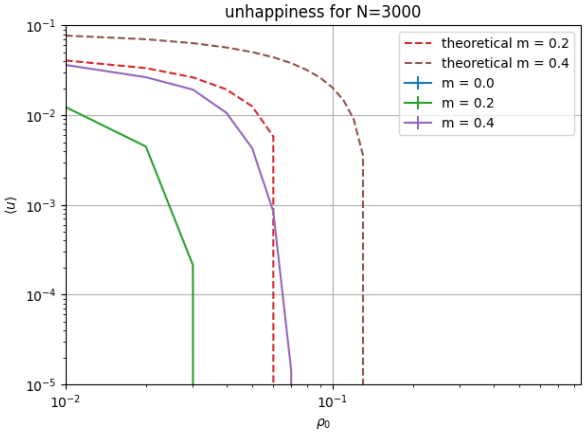

FIG. 4: Capturing the dynamics of the unhappiness coefficient as a function of various vacancy densities, with a constant grid size of $N = 300$, across diverse magnetization values m. The equation (3) is represented by a dashed line for different values of m. Both axis are presented in logarithmic scale.

For the magnetization value $m = 0$, the unhappiness remains consistently at zero across all densities of vacancies. This phenomenon is due to the equilibrium in the number of agents of both types. Applying the queuing method, as explained earlier, the movement of one agent often leaves a vacancy for another agent. Although, in some instances, there may be a few unhappy agents, these are only to fluctuations.

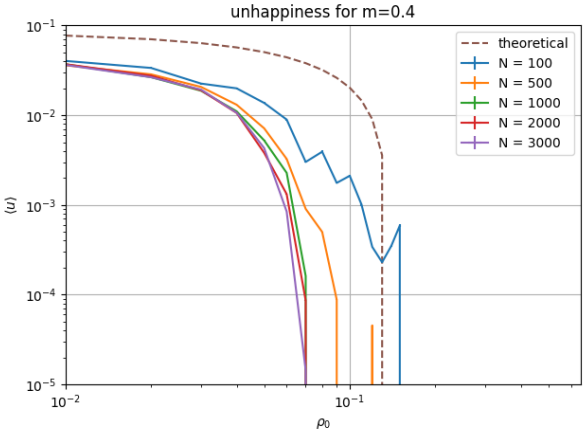

FIG. 5: Capturing the dynamics of the unhappiness coefficient as a function of various vacancy densities, with a constant magnetization value of $m = 0.4$, across diverse grid sizes denoted by N. The equation (3) is represented by a dashed line. Both axis are presented in logarithmic scale.

In contrast, for magnetization values $m \neq 0$, the number of unhappy agents escalates at low vacancy densities

with the increase of m. This is a consequence of the difference in the number of agents of different types, as elucidated in the queuing method. When there is an imbalance in the agent numbers, the minority group ends up unhappy if the number of vacancies is insufficient to create sites separated from the other type of agents. This effect gradually diminishes with the increase in the size of the grid.

The impact of finite-size can be observed in Fig. 5. As the number of sites in the grid increases, the unhappiness value slightly decreases. Similar to the segregation case, while it might initially appear that unhappiness reaches a certain value of ρ_0, where it goes to zero, as the grid size expands, definitive conclusions regarding finite-size effects cannot be drawn, as the largest studied number may still not be sufficiently large.

As noted earlier, there exists a certain value ρ_0^* where the unhappiness value goes to zero. This shift in behavior is both abrupt and continuous, potentially indicating the presence of a second-order transition. To ascertain whether this signifies a phase transition, a more thorough investigation of its behavior is imperative.

Additionally, in both figures, a plot of the theoretical approximation calculated in equation (3) is included. It is evident that its values and those of the simulation do not coincide. As mentioned with the queuing method, this is merely an approximation. This discrepancy is also observable in [6], where the values of unhappiness and the density of vacancies where the transition happens differ by the same amount as with our values.

IV. CONCLUSIONS

In this investigation, we explored a 1D variant of the original Schelling model, examining the behavior of two crucial coefficients—segregation and unhappiness—across varying vacancy densities. Our simulations encompassed a range of grid sizes and magnetization values. Both coefficients exhibited finite-size effects, with their values diminishing as the number of available sites increased. However, drawing decisive conclusions necessitates further simulations with more extensive grids.

Regarding phase transitions, indications suggest the occurrence of some form of transition in both parameters. To gain a more profound understanding of the transition type and its characteristics, an exploration of additional parameters, such as susceptibility, is imperative.

V. APPENDIX

If you would like to see the script created to run the simulations, it can be found at the next URL:
`https://github.com/SintayehuAndreu/TFG`

Acknowledgments

I would like to thank my advisor Emanuele Cozzo for his invaluable guidance, profound knowledge, and unwavering patience throughout this research journey. My gratitude also goes to my family and friends, whose support has been a pillar during crucial moments.

[1] Frank Schweitzer, Sociophysics, Physics Today 71, 2, 40 (2018)
[2] Thomas C. Schelling, Dynamic models of segregation, The Journal of Mathematical Sociology, 1:2, 143-186 (1971)
[3] Jensen, P. (2022). Introducing simple models of social systems. American Journal of Physics, 90(6), 462-468.
[4] Gauvin, L., Vannimenus, J., & Nadal, J. P. (2009). Phase diagram of a Schelling segregation model. The European Physical Journal B, 70, 293-304.
[5] Sobkowicz, P. (2007). Simple queueing approach to segregation dynamics in Schelling model. arXiv preprint arXiv:0712.3027.
[6] Dall'Asta, L., Castellano, C., & Marsili, M. (2008). Statistical physics of the Schelling model of segregation. Journal of Statistical Mechanics: Theory and Experiment, 2008(07), L07002.